SUPPLEMENTARY INFORMATION 2

On the Mechanism of the Copper-Catalyzed Enantioselective 1,4-Addition of Grignard Reagents to α, β-Unsaturated Carbonyl Compounds

Syuzanna R. Harutyunyan, Fernando López, Wesley R. Browne, Arkaitz Correa, Diego Peña, Ramon Badorrey, Auke Meetsma, Adriaan J. Minnaard,* Ben L. Feringa*

Department of Organic Chemistry and Molecular Inorganic Chemistry, Stratingh Institute, University of Groningen, Nijenborgh 4, 9747 AG, Groningen, The Netherlands

E-mail: B.L.Feringa@ rug.nl

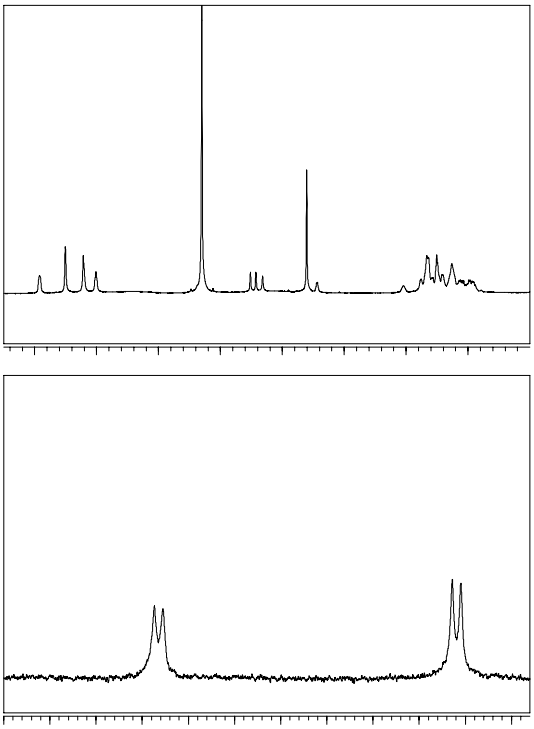

Figure S1. ^{1}H (left) and ^{31}P (right) NMR spectra of the complex **1a** in CD_2Cl_2 at -60 ^{0}C.

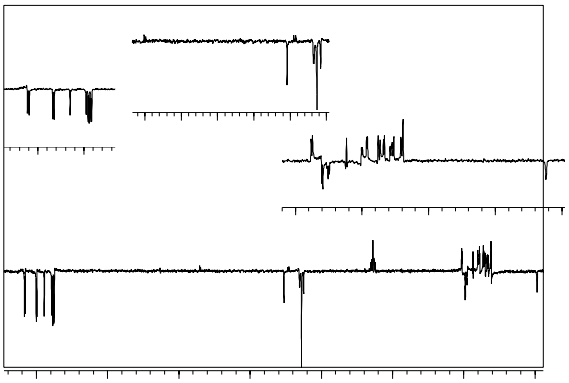

Figure S2. APT NMR (100.57 MHz) spectra of the complex **1a** in CD_2Cl_2 at RT.

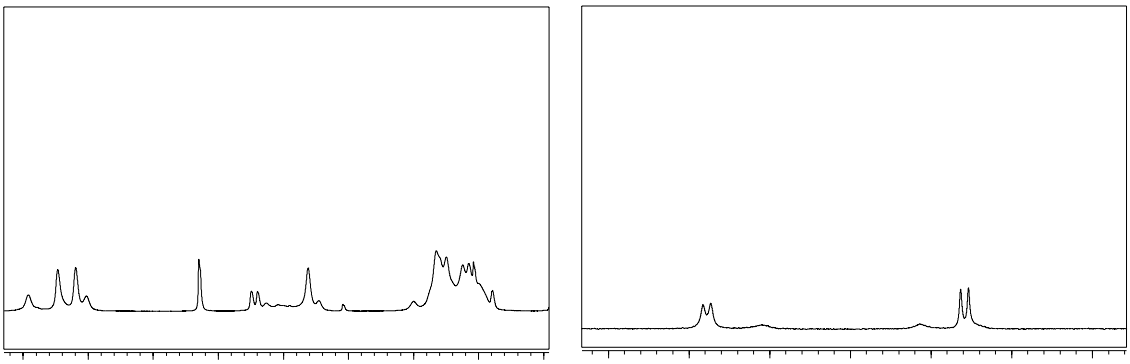

Figure S3. ^{1}H (left) and ^{31}P (right) NMR spectra of the complex **1b** in CD_2Cl_2 at -60 ^{0}C.

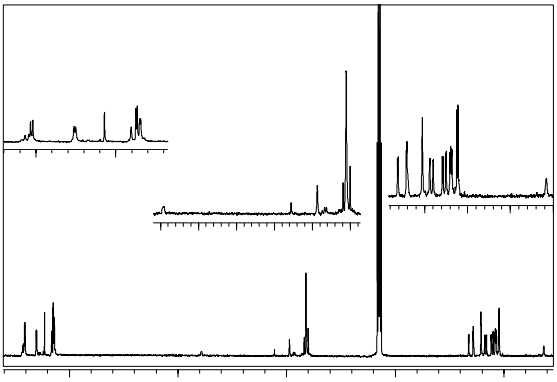

Figure S4. ^{13}C NMR (125.7 MHz) spectra of the complex **1b** in CD_2Cl_2 at RT .

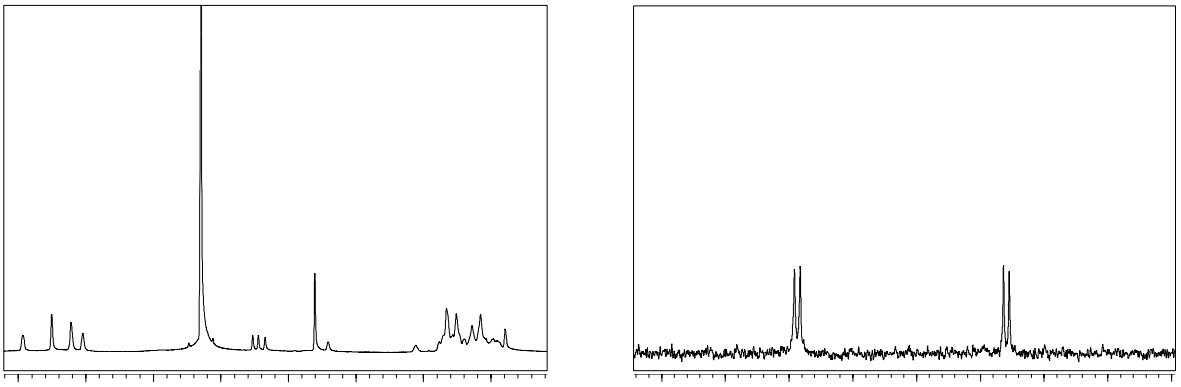

Figure S5. ^{1}H (left) and ^{31}P (right) NMR spectra of the complex **1c** in CD_2Cl_2 at -60 ^{0}C.

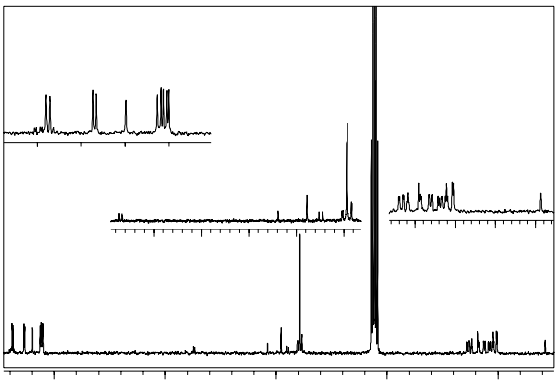

Figure S6. ^{13}C NMR (76.43 MHz) spectra of the complex **1c** in CD_2Cl_2 at RT .

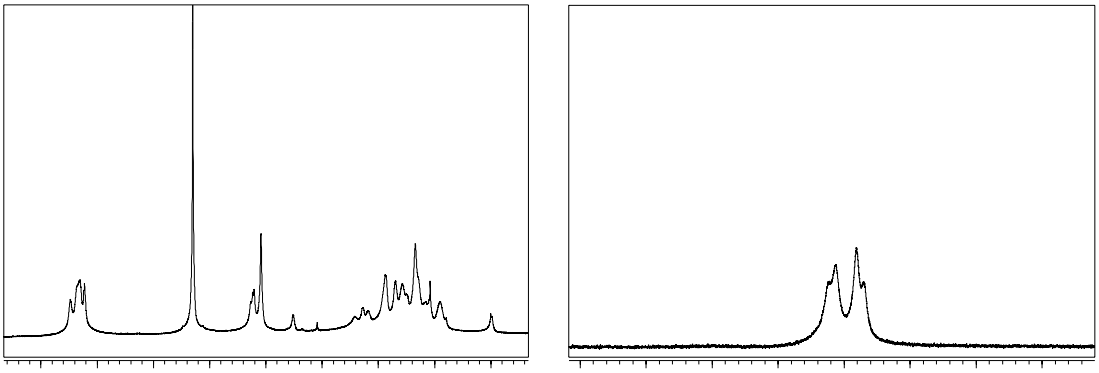

Figure S7. ^{1}H (left) and ^{31}P (right) NMR spectra of the complex **2a** in CD_2Cl_2 at -60 ^{0}C.

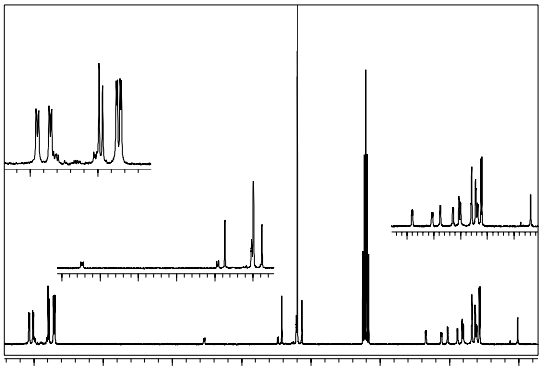

Figure S8. ^{13}C NMR (76.43 MHz) spectra of the complex **2a** in CD_2Cl_2 at RT .

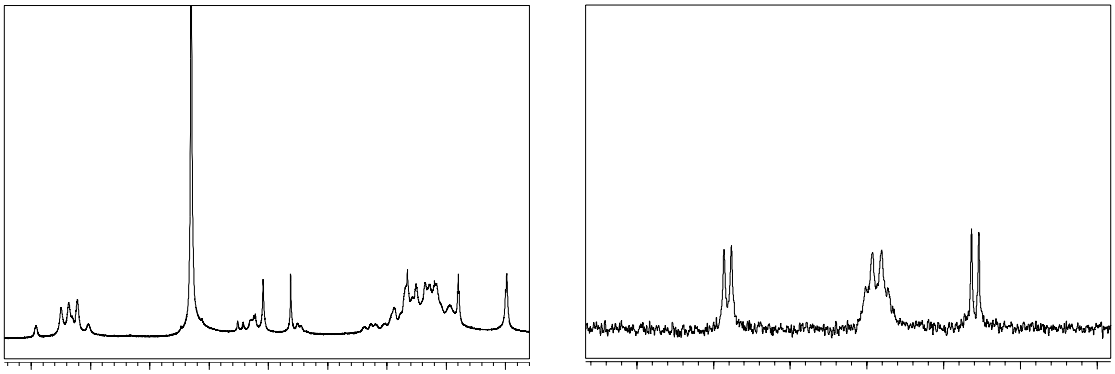

Figure S9. ^{1}H (left) and ^{31}P (right) NMR spectra of the complex **3** in CD_2Cl_2 at RT.

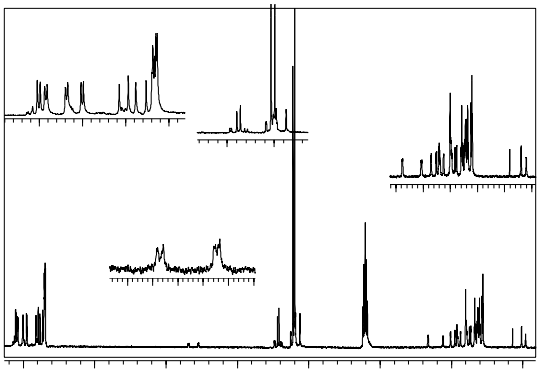

Figure S10. ^{13}C NMR (76.43 MHz) spectra of the complex **3** in CD_2Cl_2 at RT .

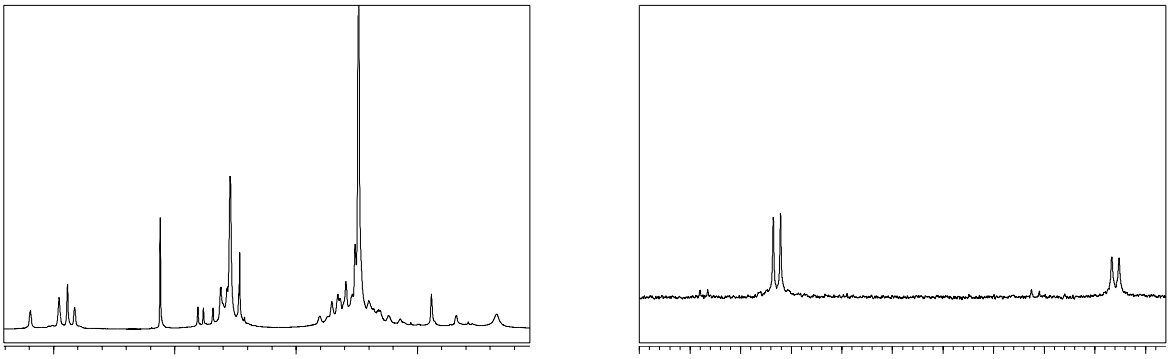

Figure S11. ^{1}H (left) and ^{31}P (right) NMR spectra of the complex **1a** and MeMgBr in CD_2Cl_2 at -60 ^{0}C.

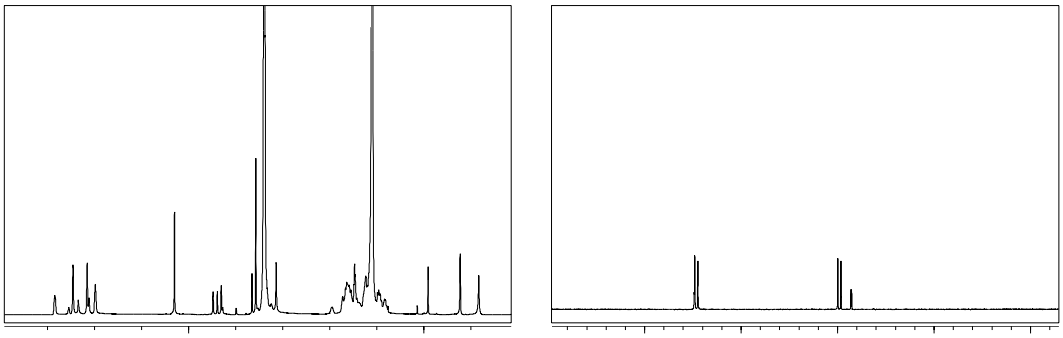

Figure S12. ^{1}H (left) and ^{31}P (right) NMR spectra of the complex **1a** and MeLi (3equiv.) in CD_2Cl_2 at -60 ^{0}C.

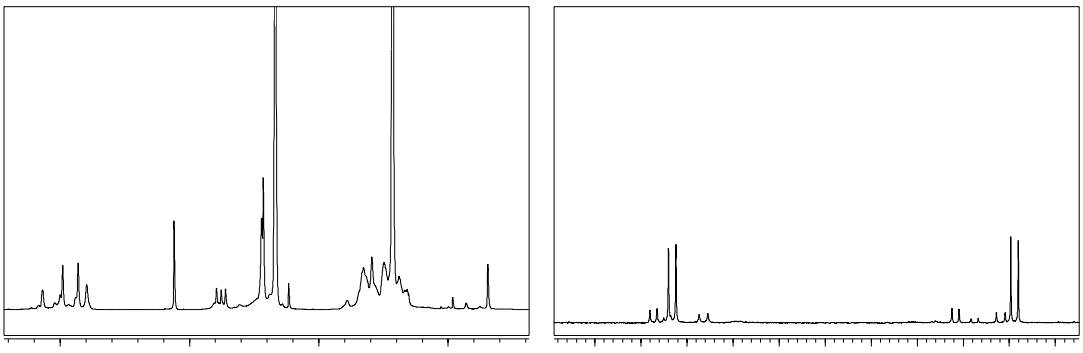

Figure S13. ^{1}H (left) and ^{31}P (right) NMR spectra of the complex **1a,** 3 equiv. of MeMgBr and 3 equiv. dioxane in CD_2Cl_2 at -60 ^{0}C.

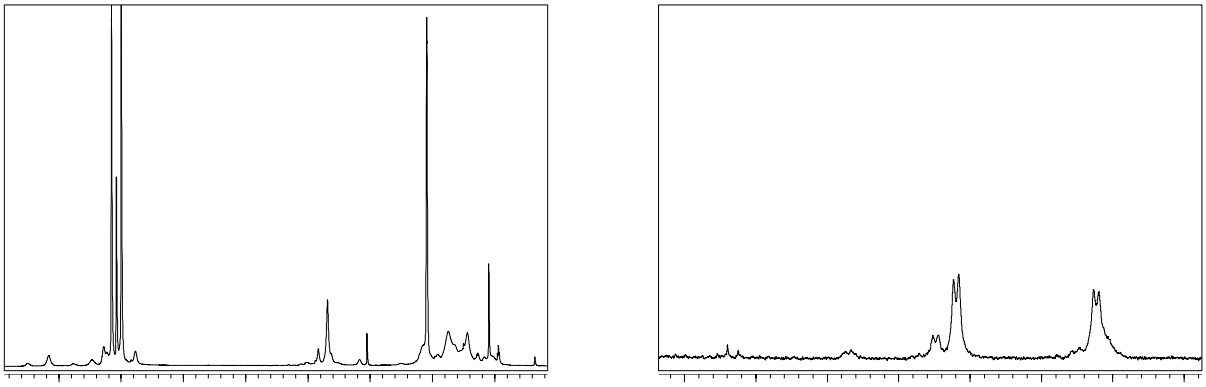

Figure S14. ^{1}H (left) and ^{31}P (right) NMR spectra of the complex **1a** in toluene-d_8 at -60.

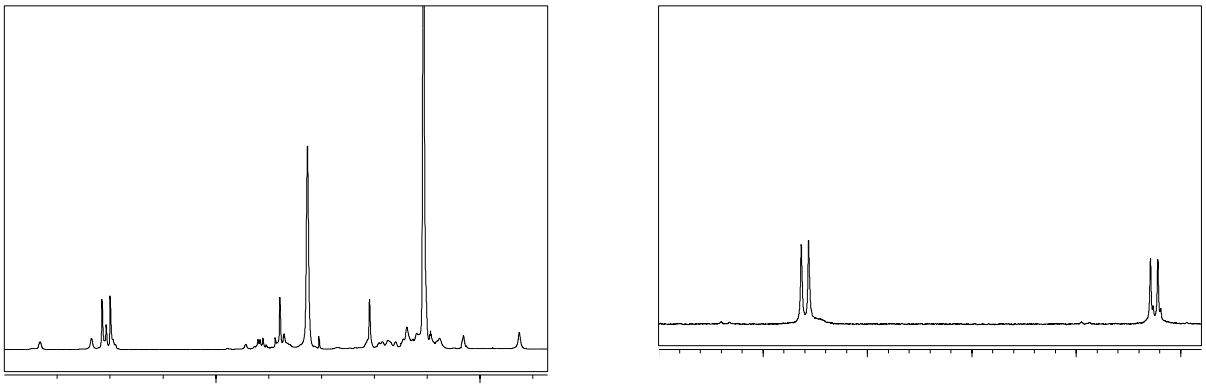

Figure S15. ^{1}H (left) and ^{31}P NMR spectra of the complex **1a** and MeMgBr in toluene-d_8 at -60 ^{0}C.

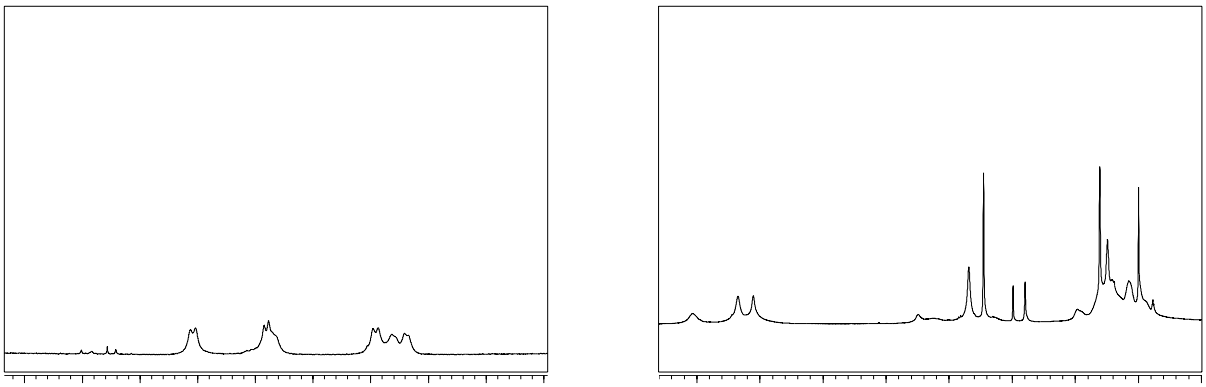

Figure S16. ^{1}H (left) and ^{31}P NMR spectra of the complex **1a** in THF-d_8 at -60.

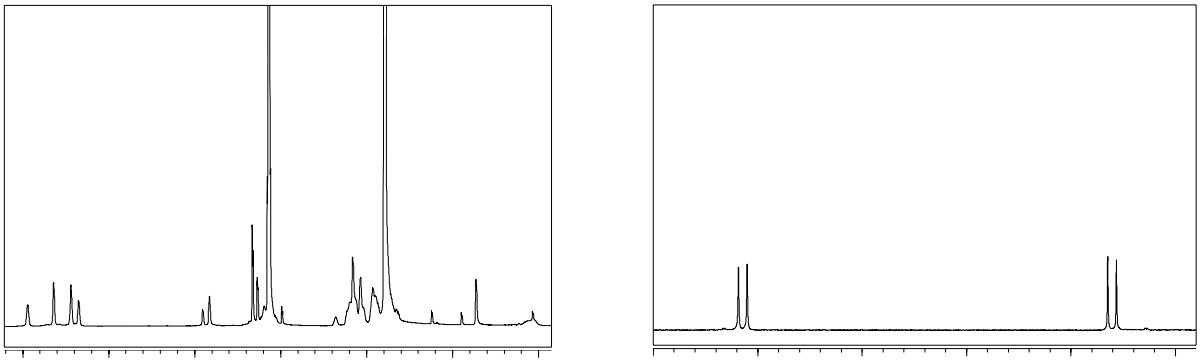

Figure S17. ^{1}H (left) and ^{31}P NMR spectra of the complex **1a** and MeMgBr in THF-d_8 at -60.

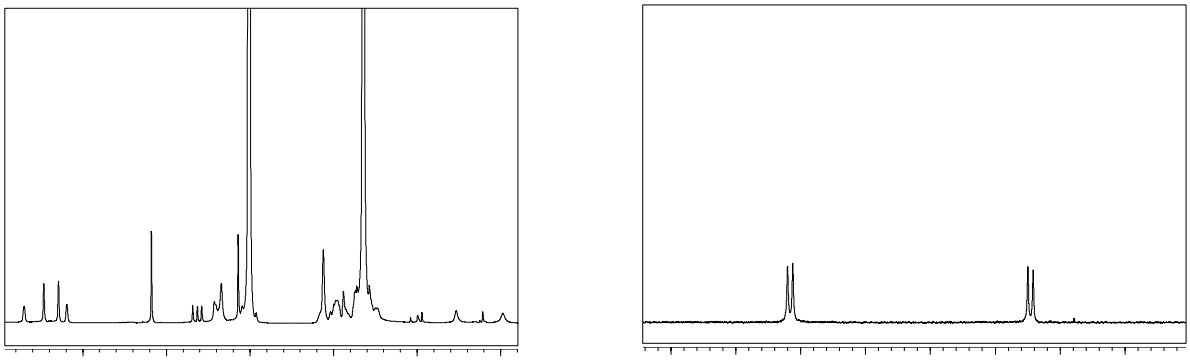

Figure S18. ^{1}H (left) and ^{31}P NMR spectra of the complex **1b** and MeMgCl in CD_2Cl_2 at -60.

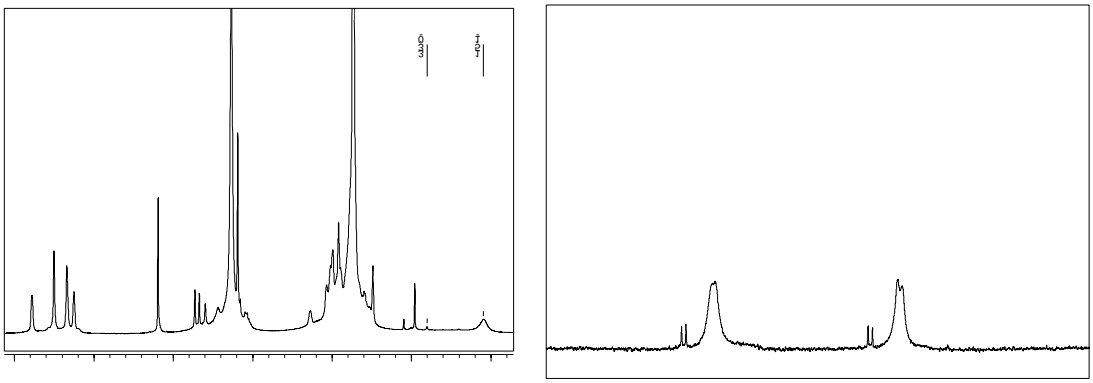

Figure S19. ^{1}H (left) and ^{31}P NMR spectra of the complex **1c** and MeMgI in CD_2Cl_2 at -60.

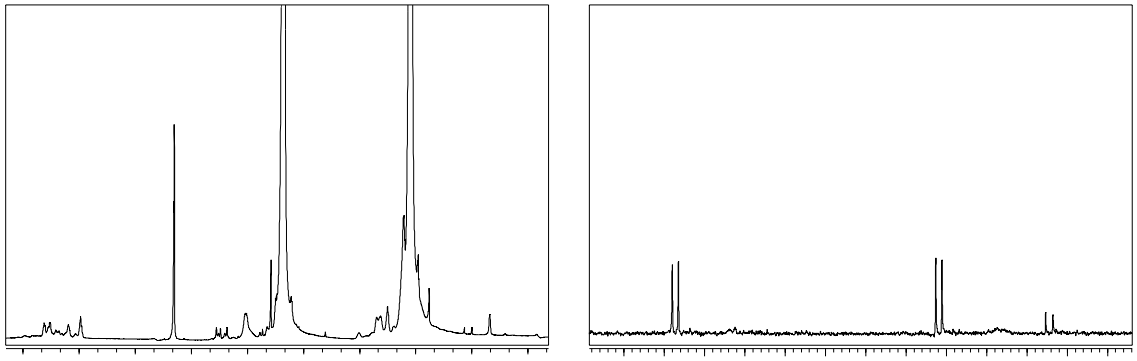

Figure S20. ^{1}H (left) and ^{31}P NMR spectra of the species **B** formed from **A** in CD_2Cl_2 at -60.